High-speed confocal fluorescence lifetime imaging microscopy (FLIM) with the analog mean delay (AMD) method

Youngjae Won,[1] Sucbei Moon,[1] Wenzhong Yang,[1] Donguk Kim,[1] Won-Taek Han,[1] and Dug Young Kim[2,*]

[1]*Department of Information and Communications, Gwangju Institute of Science and Technology, 1 Oryong-dong, Buk-gu, Gwangju 500-712, South Korea*
[2]*Department of Physics, Yonsei University, 262 Seongsanno, Seodaemun-gu, Seoul 120-749, South Korea*
**dykim1@yonsei.ac.kr*

Abstract: We demonstrate a high-speed confocal fluorescence lifetime imaging microscopy (FLIM) whose accuracy and photon economy are as good as that of a time-correlated single photon counting (TCSPC). It is based on a new lifetime determination scheme, the analog mean delay (AMD) method. Due to the technical advantages of multiple fluorescence photon detection capability, accurate lifetime determination scheme and high photon detection efficiency, the AMD method can be the most effective method for high-speed confocal FLIM. The feasibility of real-time confocal FLIM with the AMD method has been demonstrated by observing the dynamic reaction of calcium channels in a RBL-2H3 cell with respect to 4αPDD stimulus. We have achieved the photon detection rate of 125 times faster than a conventional TCSPC based system in this experiment.

OCIS codes: (000.2170) Equipment and techniques; (170.0110) Imaging systems; (170.1790) Confocal microscopy; (170.2520) Fluorescence microscopy; (170.3650) Lifetime-based sensing; (170.6920) Time-resolved imaging.

References and links

1. H. C. Gerristen, A. Draaijer, D. J. van den Heuvel, and A. V. Agronskaia, "Fluorescence lifetime imaging in scanning microscopy," in *Handbook of Biological Confocal Microscopy, 3rd Ed.*, James B. Pawley, ed. (Springer, 2006).
2. P. I. H. Bastiaens, and A. Squire, "Fluorescence lifetime imaging microscopy: spatial resolution of biochemical processes in the cell," Trends Cell Biol. **9**(2), 48–52 (1999).
3. J. Neefjes, and N. P. Dantuma, "Fluorescent probes for proteolysis: tools for drug discovery," Nat. Rev. Drug Discov. **3**(1), 58–69 (2004).
4. H.-J. van Manen, P. Verkuijlen, P. Wittendorp, V. Subramaniam, T. K. van den Berg, D. Roos, and C. Otto, "Refractive index sensing of green fluorescent proteins in living cells using fluorescence lifetime imaging microscopy," Biophys. J. **94**(8), L67–L69 (2008).
5. R. K. Benninger, O. Hofmann, B. Onfelt, I. Munro, C. Dunsby, D. M. Davis, M. A. Neil, P. M. French, and A. J. de Mello, "Fluorescence-lifetime imaging of DNA-dye interactions within continuous-flow microfluidic systems," Angew. Chem. Int. Ed. Engl. **46**(13), 2228–2231 (2007).
6. A. Esposito, T. Tiffert, J. M. A. Mauritz, S. Schlachter, L. H. Bannister, C. F. Kaminski, and V. L. Lew, "FRET imaging of hemoglobin concentration in Plasmodium falciparum-infected red cells," PLoS ONE **3**(11), e3780 (2008).
7. H. Wallrabe, and A. Periasamy, "Imaging protein molecules using FRET and FLIM microscopy," Curr. Opin. Biotechnol. **16**(1), 19–27 (2005).
8. W. Becker, A. Bergmann, M. A. Hink, K. König, K. Benndorf, and C. Biskup, "Fluorescence lifetime imaging by time-correlated single-photon counting," Microsc. Res. Tech. **63**(1), 58–66 (2004).
9. T. H. Chia, A. Williamson, D. D. Spencer, and M. J. Levene, "Multiphoton fluorescence lifetime imaging of intrinsic fluorescence in human and rat brain tissue reveals spatially distinct NADH binding," Opt. Express **16**(6), 4237–4249 (2008), http://www.opticsinfobase.org/abstract.cfm?URI=oe-16-6-4237.
10. W. Becker, A. Bergmann, H. Wabnitz, D. Grosenick, and A. Liebert, "High count rate multichannel TCSPC for optical tomography," Proc. SPIE **4431**, 249–254 (2001).
11. A. Esposito, H. C. Gerritsen, and F. S. Wouters, "Optimizing frequency-domain fluorescence lifetime sensing for high-throughput applications: photon economy and acquisition speed," J. Opt. Soc. Am. A **24**(10), 3261–3273 (2007).

#138580 - $15.00 USD Received 24 Nov 2010; revised 28 Jan 2011; accepted 28 Jan 2011; published 7 Feb 2011

12. J. Philip, and K. Carlsson, "Theoretical investigation of the signal-to-noise ratio in fluorescence lifetime imaging," J. Opt. Soc. Am. A **20**(2), 368–379 (2003), http://www.opticsinfobase.org/josaa/abstract.cfm?uri=josaa-20-2-368.
13. S. Moon, Y. Won, and D. Y. Kim, "Analog mean-delay method for high-speed fluorescence lifetime measurement," Opt. Express **17**(4), 2834–2849 (2009), http://www.opticsinfobase.org/abstract.cfm?uri=oe-17-4-2834.
14. C. E. Shannon, "Communication in the presence of noise," Proc. IRE **37**(1), 10–21 (1949).
15. ISS, Inc, "Lifetime data of selected fluorophores," *http://www.iss.com/resources/fluorophores.html*.
16. K. Yoshiki, H. Azuma, K. Yoshioka, M. Hashimoto, and T. Araki, "Finding of Optimal Calcium Ion Probes for Fluorescence Lifetime Measurement," Opt. Rev. **12**(5), 415–419 (2005).
17. H. Watanabe, J. B. Davis, D. Smart, J. C. Jerman, G. D. Smith, P. Hayes, J. Vriens, W. Cairns, U. Wissenbach, J. Prenen, V. Flockerzi, G. Droogmans, C. D. Benham, and B. Nilius, "Activation of TRPV4 channels (hVRL-2/mTRP12) by phorbol derivatives," J. Biol. Chem. **277**(16), 13569–13577 (2002).

1. Introduction

Fluorescence lifetime imaging microscopy (FLIM) is a powerful functional imaging technique in life science because of its ability to visualize localized environmental conditions, such as pH, ion concentration, refractive index, and the occurrence of fluorescence resonance energy transfer (FRET) [1–7]. High-speed confocal FLIM system is preferred in many biological studies such as protein-protein interactions or the dynamic reactions of a cell with respect to external stimuli. However, there exist many technical obstacles to be overcome for the realization of real-time confocal FLIM before it can be practically adapted in biomedical sciences. Time-correlated single-photon counting (TCSPC) and phase fluorometry methods are two well accepted standard schemes used in confocal FLIM systems. Especially, the TCSPC method is considered to be the most accurate confocal lifetime determination technique from the early days of lifetime imaging [8–10]. However, the slow photon detection rate of the TCSPC scheme is considered to be the major problem for realization of high-speed confocal FLIM. Due to the requirement of single photon arrival condition in the TCSPC method, a photon counting rate of 1 MHz can be obtainable even when a pulsed laser of 80 MHz repetition rate is employed [8]. It took more than 1 seconds to obtain an image with 128✖128 pixels, where only 61 photons for lifetime determination were for each pixel. The lifetime accuracy in this case may poor, and more photons are needed to increase lifetime accuracy, which would result in longer measurement time. Even though there is no fundamental limitation for the photon counting rate in frequency domain FLIM (FD-FLIM) techniques, there exists a practical limitation associated with nonlinear response of fluorophores at high modulation rates [11]. Photon economy which represents the detection efficiency of fluorescence photons in a FLIM system is quantified by a figure of merit F with

$$F = \sqrt{N}\sigma_\tau / \tau \tag{1}$$

where σ_τ is the standard deviation in repeated measurements of a lifetime, N is the number of photons used, and τ is the lifetime [1,12]. We have $F \geq 1$ in all lifetime measurement methods, and the closer the value to unity, the better the performance of a FLIM system. The minimum F-value for the frequency domain FLIM method with sinusoidally modulated light has reported to be 3.77[12]. When F = 3.77 the number of photons required to have a certain signal-to-noise ratio (SNR) is about 14 ($\approx 3.77^2$) times higher than that of an ideal lifetime measurement system, and there are many needs for the realization of a high-speed FLIM with high photon economy. It is reported that the F-value of a FD-FLIM can be enhanced up to 1.55 by using Gaussian-like excitation pulses having a full width at half maximum (FWHM) of 7 ns, where it also showed a very good photon efficiency [12].

We have previously introduced a new high-speed lifetime determination technique called the analog mean delay (AMD) method and demonstrated its advantages of short measurement time and high photon detection efficiency [13]. The basic principle of the AMD method is very simple; fluorescence probes are excited with a short optical excitation pulse, and the time-domain waveform of emitted fluorescence light is detected with a slow detector. Assuming that the temporal waveform of emitted light is an exponential decaying function,

#138580 - $15.00 USD Received 24 Nov 2010; revised 28 Jan 2011; accepted 28 Jan 2011; published 7 Feb 2011

the lifetime of a fluorescence probe can be extracted simply by subtracting the mean-delay of an instrument response from the mean-delay of a fluorescence signal [13]. The mathematical expression of this relation can be written as

$$\tau = < T_e > - < T_e^{\,0} > \equiv \left(\frac{\int t \cdot i_e(t) dt}{\int i_e(t) dt} \right) - \left(\frac{\int t \cdot i_{irf}(t) dt}{\int i_{irf}(t) dt} \right) \tag{2}$$

where $i_e(t)$ is a measured fluorescence signal, and $i_{irf}(t)$ is the impulse response function (IRF) of a measurement system. $< T_e >$ and $< T_e^{\,0} >$ are defined as the mean-delay of the fluorescence signal and the mean-delay of the IRF, respectively. A fluorescence lifetime can be extracted from an analog fluorescence pulse signal. Here, we assumed that the intensity of fluorescence light follows an exponential decaying form of $i(t) = Ae^{-t/\tau}$, where A is a constant. The major advantage of this method is that the mean delay effect caused by a slow measurement system can be completely removed by measuring $< T_e^{\,0} >$ from the IRF of a measurement system.

Compared to the conventional TCSPC method, the AMD method can detect multiple photons simultaneously for a single excitation pulse, and consequently the measurement speed can be very fast. Moreover, accuracy in lifetime determination and photon detection economy of the AMD method are as good as that of a TCSPC method such that the AMD method can be the most effective method for high-speed confocal FLIM. In this paper, we have extended our previous single point lifetime determination for demonstration of high speed AMD method to a real-time FLIM imaging for a cell. Our results demonstrated the feasibility of high-speed confocal FLIM with the AMD method (AMD-FLIM) by observing the dynamic reaction of calcium channels in a live RBL-2H3 cell with the addition of 4αPDD stimulus. The imaging speed of our system was achieved by 7.7 frames per second for a FLIM image of 158✖127 pixels. We achieved the photon detection rate of 125 MHz in this experiment and this is about 125 times faster than the photon detection rate of a conventional TCSPC based system. This is a first practical demonstration of the AMD-FLIM method, and we anticipate that our results may trigger the usage of the confocal AMD-FLIM technique in many biomedical functional imaging applications.

We have experimentally demonstrated that this technical achievement for high-speed FLIM imaging is attributed to the fundamental advantages of AMD method, a highly accurate lifetime determination procedure, multiple photon detection capability, and very good photon detection economy. The photon detection economy of our AMD-FLIM setup was evaluated by the *F*-value of our system. It is experimentally shown that the *F*-value of our AMD-FLIM setup is closed to the ideal value of 1 by testing the lifetime of a well-known fluorescence probe of Alexa fluor 488 whose lifetime is known to be 4.1 ns. The multiple photon detection capability of our setup was shown by plotting a linearity relation between the number of detected photons versus measured electronic voltage by our detection system. And, the highly accurate lifetime determination procedure in the AMD-FLIM setup was verified by monitoring uncertainties in measured lifetime versus the number of photons used for lifetime determination. Another very important advantage of the AMD lifetime measurement method is that the precision of measured lifetime can be much better than the actual bandwidth of a measurement system. This becomes possible by assuming the temporal waveform of measured fluorescence intensity is a simple exponential function. We have shown that high precision lifetime information can be extracted from low bandwidth data by using a series of numerical simulations.

#138580 - $15.00 USD Received 24 Nov 2010; revised 28 Jan 2011; accepted 28 Jan 2011; published 7 Feb 2011

2. Experiments and results

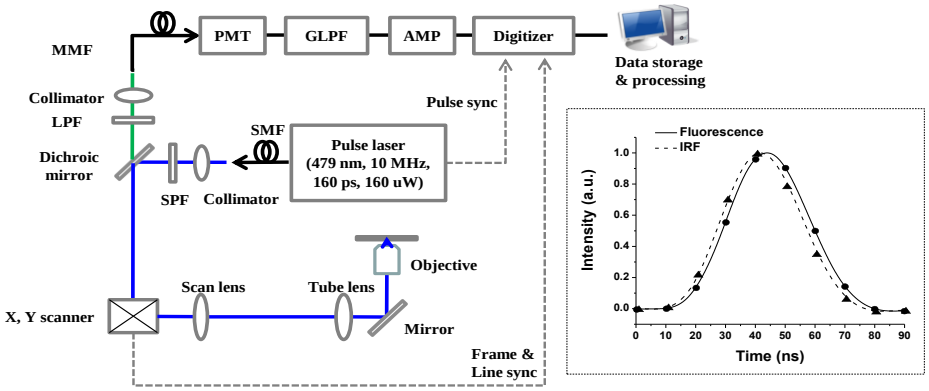

Fig. 1. Schematic diagram of high-speed confocal FLIM by the AMD method.

Figure 1 shows the schematic diagram of a point scanning confocal FLIM system with the AMD method. A gain-switched diode laser (PicoQuant, LDH-P-C-485) operating at 479 nm wavelength with 10 MHz pulse repetition rate is used as the excitation laser source. Laser pulses of 160 ps duration with an average power of 160 µW are delivered through a single mode fiber (SMF) to a collimator. Collimated laser beam passes through an optical short-pass filter (SPF) with a cut-on wavelength of 485 nm to cut unwanted spontaneous emission wavelength components in the laser. After the excitation laser beam is reflected by a dichroic mirror with 505 nm cut-off wavelength, it is scanned by a resonant scanner (GSI, CRS4KHz) at a frequency of 4 kHz for horizontal scanning and by a moving magnet scanner (GSI, VM500S) for vertical image formation. The vertical scanner was set to scan one cycle in every 256 periods of the horizontal scanner. The laser beam is focused on a sample with a 60X objective lens (Olympus, NA 0.8). Fluorescence signal from a sample is transmitted through the dichroic mirror and is further filtered by an optical long-pass filter (LPF) with a cut-on wavelength of 490 nm. A multimode fiber (MMF) with a core diameter of 10 um is used as a pin-hole in a confocal system and is connected to a photomultiplier tube (PMT, Hamamatsu, R7400U-20). Electric pulse signal from the PMT is temporally broaden by a home-made 10th Gaussian low-pass filter (GLPF) before it is amplified by an electric amplifier (Minicircuits, TB-409). Amplified electric signal is taken by a digitizer (National Instruments, PCI-5114) with 8 bit resolution at 100 MHz sampling rate, which is fast enough to handle a signal whose highest frequency component is 50 MHz. The internal clock of the digitizer was phase-locked with that of the pulsed laser source. The bandwidth of used digitizer is 200 MHz and it is very suitable to handle the signal whose frequency components are less than 50 MHz. We have experimentally verified that the temporal jitter of the digitizing window of our digitizer is about 20 ps. For the real-time recording of fluorescence signals, we have adopted a DAQ board with high-speed PCI interface, and a redundant array of independent disks (RAID) system is employed for real-time data streaming from the digitizer to hard disks in a personal computer (PC).

There are many advantages of broadening a fast decaying exponential function with an analog Gaussian low-pass filter before it is digitized with a data acquisition (DAQ) board. The broadened signal can be easily handled with cost effective electronic components such as low-bandwidth amplifiers, DAQ boards and standard data storage devices. By the Nyquist-Shannon sampling theorem, an original signal can be perfectly reconstructed when the sampling frequency is more than twice of the highest frequency of an original signal [14]. We added a home-made electric Gaussian low pass filter (GLPF) after PMT to make the highest frequency of the IRF signal become less than 50 MHz. The 50 MHz cut-off frequency was chosen to avoid aliasing in the digitizer whose sampling rate was 100 MB/s. The pulse

#138580 - $15.00 USD Received 24 Nov 2010; revised 28 Jan 2011; accepted 28 Jan 2011; published 7 Feb 2011

repetition rate of 10 MHz was chosen to maximize the measurement speed while keeping adjacent pulses apart in the time domain. If we had a faster digitizer, we could use an anti-aliasing filter with higher 70 dB cut-off frequency. Then, the repetition rate of the pulsed laser can be higher, and the overall measurement speed can be faster. Due to this, the original signal whose highest frequency component is less than 50 MHz could be perfectly reconstructed by the DAQ board with a sampling rate of 100 MHz. From the mathematical expressing shown in Eq. (2), the extra mean delay $< T_e^0 >$ generated by this low-pass filter can be perfectly eliminated from a measured mean delay $< T_e >$ to obtain the mean delay of a fluorescence probe τ. By doing a series of numerical simulations, we have shown that the accuracy in the mean delay obtained by the AMD method is not lost by the low-pass filter in our measurement system. Despite large sampling interval of 10 ns in our measured data, we have shown that the fluorescence lifetime is well extracted.

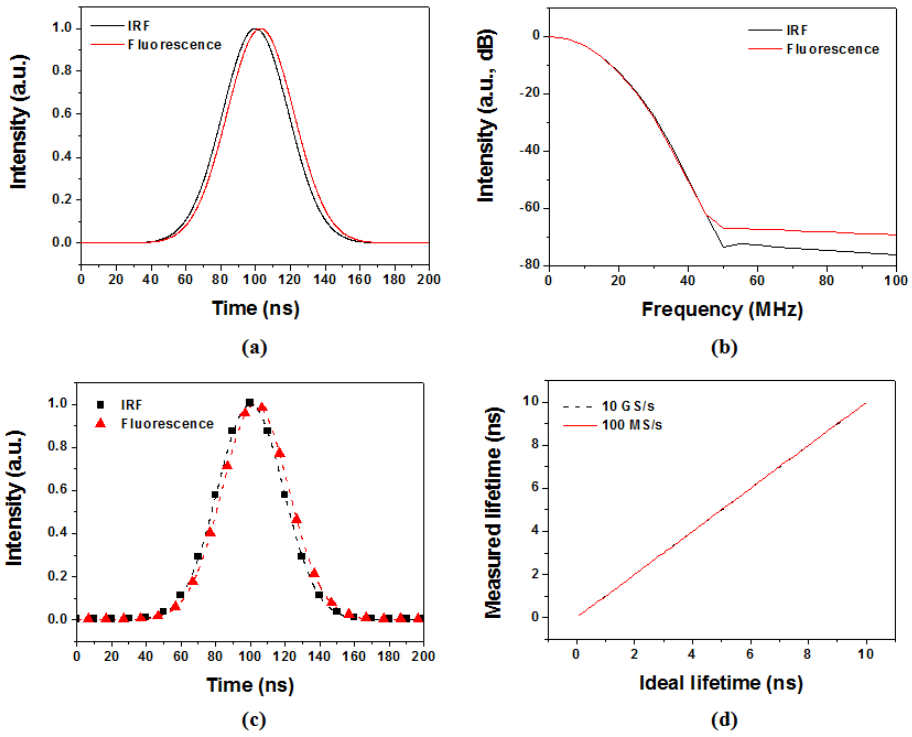

Fig. 2. (a) Simulated IRF and fluorescence signal sampled by 10 GHz, (b) Frequency components of the signals shown in (a), (c) Simulated IRF and fluorescence signal sampled by 100 MHz, (d) Lifetimes extracted by AMD method with the signals sampled by 10 GHz and 100 MHz.

Figure 2(a) represents simulated IRF (blue) and fluorescence (red) signals which can be obtained by our measurement system for an ideal exponentially decaying signal with a lifetime of 3 ns. In these numerical simulations, the IRF signal was assumed to be a Gaussian pulse with a FWHM of about 40 ns. The fluorescence signal was obtained by calculating the convolution between the ideal exponentially decaying fluorescence function and the IRF signal. Sampling frequency for the pulses shown in Fig. 2(a) is 10 GHz with a sampling interval of 0.1 ns. This is much less than typical fluorescence lifetimes which are in the order of a few ns. The frequency components of these signals are shown in Fig. 2(b). The highest frequencies of both signals are less than 50 MHz and this shows the original signal can be perfectly reconstructed by the sampling rate of 100 MHz. Figure 2(c) shows the same signal of Fig. 2(a), but sampled with a 100 MHz sampling frequency. Black square and red triangle

#138580 - $15.00 USD Received 24 Nov 2010; revised 28 Jan 2011; accepted 28 Jan 2011; published 7 Feb 2011

dots represent the IRF and the fluorescence signal, respectively. The extracted lifetimes by the AMD method with signals generated at 10 GHz and 100 MHz sampling rates are shown in Fig. 2(d) with a dotted black line and a solid red line for several different ideal lifetimes from 0.1 ns to 10 ns with an increase of 0.1 ns. It shows that the extracted lifetimes from the signal sampled at 10 GHz and those at 100 MHz are well matched with original lifetimes.

Due to the timely spreading and the electronic amplification of an original exponentially decaying signal, extra noises are introduced, which may affects lifetime determination in the AMD method. However, these noises can be effectively reduced by multiplying a window function to the original data when calculating the mean-delay of a measured signal. We have shown that the optimum size of the window is about the FWHM of the IRF signal [13]. Because the mean-delay of a Gaussian-like pulse signal is almost at the center of the pulse, the mean-delay of a signal can be accurately calculated within a small size window. However, when a waveform of 40 ns pulse width is measured with a 10 ns sampling interval, the mean-delay of the waveform calculated from the raw data does not produce consistent results because there are only 5 data points within the integration window. To obtain consistent mean-delays for repeated measurements, acquired waveform data for the IRF and the fluorescence signals were interpolated by a spline interpolation method such that sampling interval of data becomes to be 0.1 ns. Black and red dashed lines in Fig. 2(c) show these interpolated data.

We have used a non-fluorescent scattering sample to obtain the exact IRF of our measurement system. IRF was acquired with a sampling rate of 100 MHz and was later interpolated to become 10 GHz data by a spline interpolation method. Typical waveforms of an IRF $i_{irf}(t)$ and a fluorescence signal $i_e(t)$ are displayed on the right side of Fig. 1. Solid black triangles and circles are raw data points of IRF and fluorescence signal, respectively. Dashed line and solid lines represent interpolated data of each raw signal. For image construction, 1,268 excitation pulses were used for a single horizontal line, and 512 vertical lines were made with 256 cycles of forward and backward horizontal scans. In total, 1,268✖512 pulses were used to construct a single 2D image. To increase the signal-to-noise ratio (SNR), 8 neighboring pulses in the horizontal axis and 4 neighboring pulses in the vertical axis were averaged, and then two consecutive frames were averaged such that 64 pulses are used to determine the lifetime of a single image pixel. The pixel dwell time becomes 6.4 us and a single frame is composed of 158✖127 pixels. Thus, it takes less than 0.13 s to obtain a single 2D image of 158✖127 pixels. In our point-scanning confocal imaging system, the number of pixels in an image and the frame rate can be further enhanced depending on the SNR of a fluorescence signal to be measured. If fluorescence signal is high, or its SNR is good, the pixel numbers in an image frame can be increased by reducing the average number of pixels. The frame rate can be also increased by utilizing a high-speed resonant scanner as long as the SNR of fluorescence signal is high.

The accuracy and photon economy of our high-speed confocal AMD-FLIM system were checked with an artificial sample of Alexa fluor 488 (Invitrogen), and measurement results are shown in Fig. 3. 10 μM of Alexa Fluor 488 diluted by phosphate buffered saline (PBS) was dropped on a slide glass and covered with a cover slide. To estimate the number of photons detected in our measurement system in regard to different levels of measured fluorescence power, fluorescence photons were firstly counted by using a PMT and a high-speed sampling oscilloscope. By repeating the same experiments with different powers of very weak CW laser irradiation, we can obtain the ratio between the photon number and the detected optical power. Then, the photon number of detected fluorescence signal was obtained by multiplying the ratio to the measured optical power of fluorescence signal. In order to have the same condition used in a 2D FLIM image, we have used the averaged signal by neighboring 64 fluorescence pulse signals in determining a single lifetime in Fig. 3. For each given detected fluorescence power or the detected photon number in the horizontal axes of Fig. 3, 3000 lifetimes were measured and used to obtain the standard deviation (SD) of lifetime ($\sigma_\tau = \Delta\tau_{tot}$).

#138580 - $15.00 USD Received 24 Nov 2010; revised 28 Jan 2011; accepted 28 Jan 2011; published 7 Feb 2011

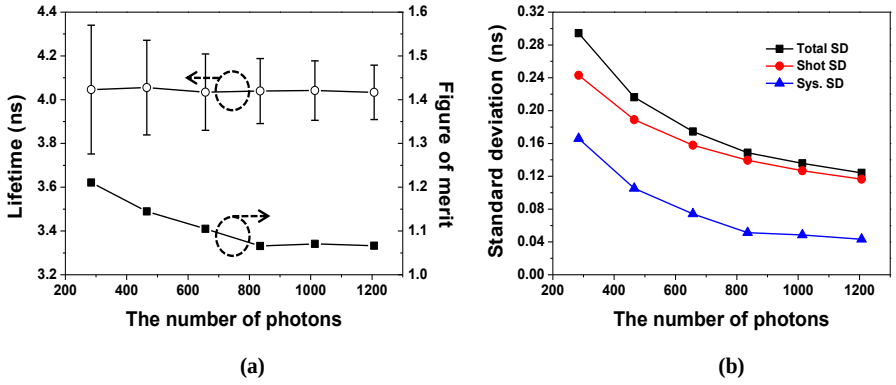

Fig. 3. (a) Fluorescence lifetime of Alexa fluor 488 and figure of merit in regard to the number of photons. (b) Standard deviation in lifetime as a function of the photon number used for lifetime measurement in our AMD-FLIM system. Total SD, Shot SD, and Sys SD represent $\Delta\tau_{tot}$, $\Delta\tau_{shot}$, and $\Delta\tau_{sys}$, respectively.

Empty blank circles and error bars in Fig. 3(a) show the averaged lifetimes and the standard deviations of Alexa fluor 488 measured by the AMD method. The averaged lifetimes were all within 4.03~4.05 ns, and these were well matched to the reported lifetime of 4.1 ns [15]. Solid black squares in Fig. 3(a) represent figure of merit (F) calculated from measured data and Eq. (1). Calculated F decreases slightly from 1.21 to 1.06 as the number of detected photons N is increased from 300 to 800. These results are compatible with that of TCSPC method and represent the excellent photon economy of our AMD-FLIM system. Two dashed circles with arrows in Fig. 3(a) are to show corresponding Y-axis of each graph.

The photon economy of our AMD-FLIM system is further investigated and shown in Fig. 3(b). Solid black squares in Fig. 3(b) show measured standard deviation ($\Delta\tau_{tot}$) of lifetime as a function of the number of photons (N) used for lifetime determination. In probability theory, the measured standard deviation of a fluorescence lifetime can be divided into the contribution from the shot noise of photons ($\Delta\tau_{shot}$) and the contribution from a measurement system ($\Delta\tau_{sys}$). Since occurrence of the shot noise and that of the system noise are not correlated with each other, this relation can be written as

$$\Delta\tau_{tot} = \sqrt{\Delta\tau_{shot}^2 + \Delta\tau_{sys}^2}. \qquad (3)$$

The ideal standard deviation due to the shot noise of photons ($\Delta\tau_{shot}$) was calculated from Eq. (1) with F = 1 ($\Delta\tau_{shot} = \tau/\sqrt{N}$). Standard deviation contributed by the system noise ($\Delta\tau_{sys}$) was obtained from Eq. (3) and the measured standard deviation ($\Delta\tau_{tot}$) for each photon number. $\Delta\tau_{shot}$ and $\Delta\tau_{sys}$ are represented by red circles and blue triangles in Fig. 3(b), respectively. As shown in Fig. 3(b), the contribution by the system noise in the standard deviation of measured lifetimes is much smaller than the contribution from the shot noise. These results show that the photon economy of our AMD-FLIM system almost reaches the ideal shot-noise limited case.

#138580 - $15.00 USD Received 24 Nov 2010; revised 28 Jan 2011; accepted 28 Jan 2011; published 7 Feb 2011

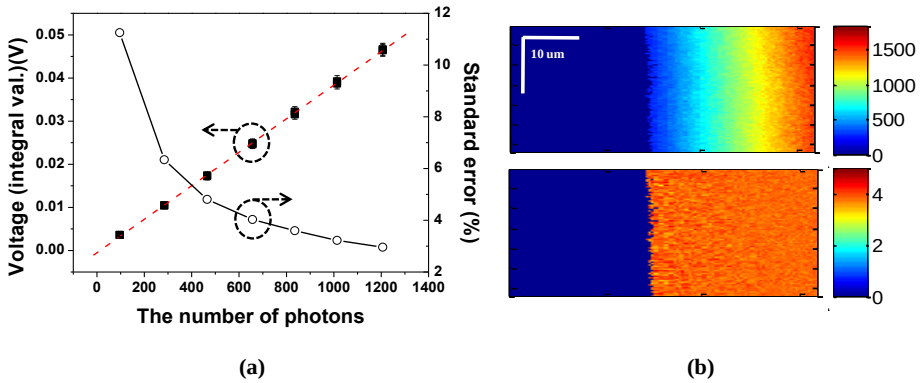

Fig. 4. (a) Calibration between intensity of analog pulse signal and the number of photons (b) Fluorescence intensity (top) and lifetime (bottom) images of Alexa fluor 488.

Since an analog fluorescence pulse signal composed with multiple photons is used in the AMD-FLIM method, a linear relation between measured voltage and number of fluorescence photons needs to estimate the number of fluorescence photons from a measured analog signal. We have verified this linear relation and the results are presented in Fig. 4(a). Integrated voltage for the top 80% of a detected signal was used as the voltage value in Fig. 4(a). We used the averaged signal with neighboring 64 fluorescence pulse signals for determination of a single integrated voltage value. The mean values of integrated voltage and corresponding standard deviations are calculated and plotted with solid black squares and error bars in Fig. 4(a) for 3000 measurements. Since 64 detected fluorescence pulse signals were used for each lifetime determination, measured voltages are linear up to about 20 photons per single fluorescence pulse signal. We estimated the number of photons from independent 3000 analog fluorescence pulse signals by the ratio obtained by linear fitting. Then we gained the standard errors for the estimated number of photons and these are also plotted with empty circles in Fig. 4(a) for various photon numbers. The standard errors for estimated number of photons larger than 4 00 were less than 5%.

Based on this, we measured the intensity and lifetime images of Alexa fluor 488. The top image of Fig. 4(b) shows fluorescence intensity and lifetime with various measured fluorescence intensities or photon numbers near the edge of the same artificial sample used in Fig. 3. The sample is a liquid drop of Alexa Fluor 488 diluted by phosphate buffered saline (PBS) on a slide glass and covered with a cover slide. Measured fluorescence intensities were converted and represented by the number of photons in Fig. 4(b). The pseudo color bar on the right side of the image represents the intensity of measured fluorescence signal for each pixel in terms of the number of measured fluorescence photons. It shows that the concentration of Alexa Fluor 488 increases continuously from a blunt vertical boundary located at the center of the image toward the right side of the image. Fluorescence lifetimes are calculated with our AMD method from the same data used in fluorescence intensity image shown at the top of Fig. 4(b), and a corresponding FLIM image is constructed and plotted at the bottom of Fig. 4(b). The pseudo color bar on the right side of the FLIM image shows the scale of lifetime in ns. Unlike the fluorescence intensity image shown at the top of Fig. 4(b), the lifetime image of the artificial Alexa fluor 488 liquid shows binary values regardless of the concentration of Alexa fluor 488. Lifetimes are calculated with less than 200 photons for some pixels near the vertical boundary at the center of the image, and there exist large fluctuations in calculated lifetime. Since the number of measured fluorescence photons per pixel becomes large on the right side of the FLIM image at the bottom of Fig. 4(b), pixel-to-pixel fluctuations in measured lifetime decreases on the right side.

#138580 - $15.00 USD Received 24 Nov 2010; revised 28 Jan 2011; accepted 28 Jan 2011; published 7 Feb 2011

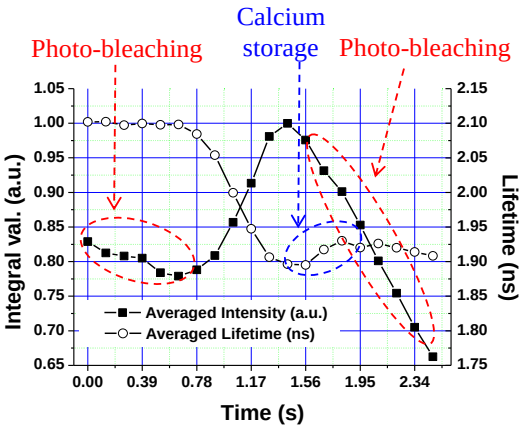

(a)

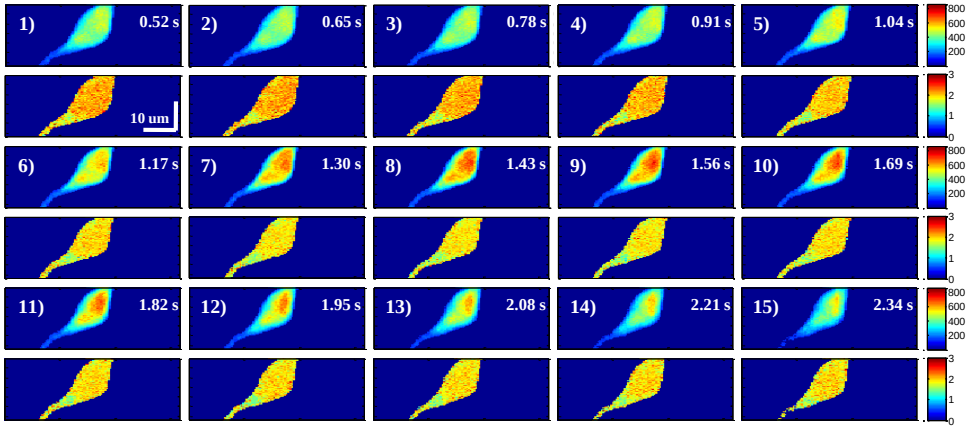

(b)

Fig. 5. Real-time dynamic FLIM images. (a) Average fluorescence intensity and lifetime variations inside a cell due calcium channel opening. (b) fluorescence intensity (top) and lifetime (bottom) images from 0.52 s to 2.34 s with frame rate of 7.7 frames/sec.

In order to demonstrate the real-time imaging capability of our AMD-FLIM system, we have measured the dynamic changes of calcium ion concentration in an RBL-2H3 cell labeled with Fluo-3 (see methods) whose fluorescence intensity increases, while its lifetime decreases as a function of calcium ion concentration [16]. Black squares and blank circles in Fig. 5(a) show the average intensity of fluorescence light and its lifetime within the RBL-2H3 cell while Ca^{2+} channels of the cell are activated 4α-phorbol 12, 13-didecanoate (4α-PDD) [17]. The activation starts at t = 0.65 s by 5 uM of 4α-PDD. Note that fluorescence intensity is decreased from t = 0 s to t = 0.65 s due to photobleaching while the average fluorescence lifetime does not change during this period. This is one of the major advantages of FLIM over fluorescence intensity imaging. Activation of Ca^{2+} channels are verified by the increase of fluorescence intensity and the decrease of lifetime starting at t = 0.65 s until t = 1.43 s. There is a continuous decrease in fluorescence intensity after t = 1.43 s, and it is also due to photobleaching. Lifetime becomes minimum at t = 1.56 s, and there is a small increase of lifetime just after this minimum point for about 0.26 seconds. We believe that this slight increase is due to calcium storage inside the cell. Since this happens within 1/3 of a second, and the amount of lifetime change is less than 0.03 ns, it is hardly observable with a conventional FLIM system. Figure 5(b) shows fifteen fluorescence intensity (top) and lifetime

#138580 - $15.00 USD Received 24 Nov 2010; revised 28 Jan 2011; accepted 28 Jan 2011; published 7 Feb 2011

images (bottom) that are used to create the plot in Fig. 5(a). Time interval between FLIM images is 0.13 s. The maximum number of photons for a single pixel was more than 800 in Fig. 5(b8). In this case, the photon detection rate was higher than 125 MHz due to the pixel dwell time of 6.4 us. Note that there are definite difference in the intensity images of Fig. 5(b8) and (b15) due to photobleaching while a little bit changes are shown in the lifetime images without any effect of photobleaching.

3. Conclusions

In summary, we have demonstrated the feasibility of a real-time confocal FLIM system and its practical usage in bioscience utilizing a new high-speed AMD lifetime determination scheme. Since multiple fluorescence photons can be simultaneously detected with a single excitation pulse in the AMD-FLIM system, we were able to obtain a very high photon detection rate of 125 MHz which is about 125 times faster than that of conventional TCSPC method. Herein, the photon detection rate of the AMD method was estimated by counting the number of fluorescence photons with a careful calibration between the average power of analog fluorescence pulses and the number of photons associated with it. The figure-of-merit F of our system is shown to be about 1.06, which is very close to the ideal shot noise limited value of 1. We have also shown that our AMD-FLIM method can be used with various levels of fluorescence power in practice with high lifetime accuracy and good photon economy. The practical application of our system were demonstrated by observing the dynamic activation of Ca^{2+} channels in a RBL-2H3 cell, where a fast frame rate of 7.7 Hz was achieved. We believe that our new AMD-FLIM method can be a breakthrough for the realization of real-time confocal FLIM with high lifetime accuracy and its practical usage in biomedical sciences.

Acknowledgments

This work was supported by the Creative Research Initiatives Program of Korea Science and Engineering Foundation (KOSEF) / Ministry of Education, Science and Technology.

#138580 - $15.00 USD Received 24 Nov 2010; revised 28 Jan 2011; accepted 28 Jan 2011; published 7 Feb 2011